Registration and Fusion of Contrast-Enhanced MRI Myocardial Substrate Maps and X-ray Angiograms

Juan E Ortuño[1,2], Esther Pérez-David[3], Ángel Arenal[3], Javier Bermejo[3], Andrés Santos[2,1], María J Ledesma-Carbayo[2,1]

[1]CIBER-BBN, Madrid, Spain
[2]Universidad Politécnica de Madrid, Spain
[3]Hospital General Universitario Gregorio Marañón, Madrid, Spain

Abstract

The aim of this work is to provide the necessary methods to register and fuse the endo-epicardial signal intensity (SI) maps extracted from contrast-enhanced magnetic resonance imaging (ceMRI) with X-ray coronary angiograms using an intrinsic registration-based algorithm to help pre-planning and guidance of catheterization procedures.

Fusion of angiograms with SI maps was treated as a 2D-3D pose estimation, where each image point is projected to a Plücker line, and the screw representation for rigid motions is minimized using a gradient descent method. The resultant transformation is applied to the SI map that is then projected and fused on each angiogram.

The proposed method was tested in clinical datasets from 6 patients with prior myocardial infarction.

The registration procedure is optionally combined with an iterative closest point algorithm (ICP) that aligns the ventricular contours segmented from two ventriculograms.

1. Introduction

X-ray fluoroscopic coronary angiograms provide high-resolution projections of the arterial coronary tree but require the use of ionizing radiation, have poor soft tissue definition, and only provide 2D projections of complex 3D anatomy. Magnetic resonance Imaging (MRI) allows 3D cardiac imaging with high contrast between healthy and nonviable tissue. Registering and fusing X-ray angiograms with cardiac MRI, combines the best features of both modalities to guide catheterization procedures and pre-operation planning [1, 2]

Contrast-enhanced magnetic resonance imaging (ceMRI), also known as delayed-enhancement MRI, has been proven to be a reliable cardiac magnetic resonance tool for differentiating between viable and nonviable tissue [2].

In ceMRI, the typical pulse sequence consists of an inversion-recovery prepared T1-weighted gradient-echo sequence after the intravenous administration of a gadolinium-chelate. The inversion-recovery sequence is used to optimize the contrast between healthy or viable myocardium and gadolinium-retaining scar tissue, which appears bright or hyper-enhanced. The heterogeneous tissue will present an intermediate level of SI.

X-ray images are obtained with a C-arm device with rotation in two axis (primary and secondary angles) and bed translation. These 2D projections are modeled as an undistorted pinhole camera model, defined by the camera transformation matrix **[R|t]** and the intrinsic matrix **K**.

The ceMRI volumetric image needs to be registered before being fused with 2D projections acquired using X-ray fluoroscopy. The most usual method consists of attaching common reference points (known as fiducial markers) to the surface of the patient, and using the correspondence of those fiducial markers to warp the rest of the images until they overlap [3].

2. Methods

2.1. Signal intensity maps

The SI map consists of a 3D surface on which the average sub-endocardial or sub-epicardial SI obtained from ceMRI is projected. The surface is parameterized as a triangulated mesh that represents either the endocardial or the epicardial surface of the left ventricle.

To obtain the SI map, the left ventricular endocardial/epicardial contours were manually defined using QMass MR Version 7.0 (MEDIS) on contiguous slices computed from the short-axis ceMRI view. These contours were imported into the mapping tool, which is described in detail in [4].

Mesh reconstruction of the left ventricle was color coded to provide information of healthy, heterogeneous and scar tissue, as well as their shapes and relative position, which could be observed at once.

2.2. 2D-3D registration

Registration and fusion of 2D angiograms with ceMRI derived 3D SI maps can be interpreted as an exterior orientation problem (also known as the camera pose problem in computer vision). The device is assumed to be calibrated, i.e., intrinsic matrix **K** is known. The C-arm position and orientation can be determined with a set of point correspondences (X_i, x_i), with 3D (model) points X_i and image points x_i.

For any three non-collinear control points X_i, the location of optical center can be found and four possible solutions are obtained [5]. Larger number of points increases the robustness of the method. A non-iterative method with n ≥ 4 give an unique solution in non degenerate cases [6].

The external orientation problem is equivalent to the estimation of a rigid body motion [7] as detailed in the following section.

2.3. Rigid motion

Each image point is reconstructed to a Plücker line $L_i = (n_i, m_i)$ with direction n_i and moment m_i [8]. The rigid motion is represented as an exponential form $\mathbf{M} = \exp(\theta\hat{\varepsilon})$, where $\theta\hat{\varepsilon}$ is the matrix representation of a twist ε. A twist contains six parameters; three of them correspond to the motion velocity. By varying θ, the motion can be identified as screw motion around an axis in space. **M** can be computed efficiently using the Rodriguez formula [8].

Incidence of the transformed 3D point X_i with the Plücker line L_i can be expressed as:

$$(\exp(\theta\hat{\varepsilon})\, X_i)_{3\times 1} \times n_i - m_i = 0 \qquad (1)$$

After multiplying matrix **M** with the vector X_i (in homogeneous coordinates), the homogeneous component is neglected. This constraint equation expresses the perpendicular error vector between the Plücker line and the point X_i. The equation (1) is linearized using the two first term of the Taylor expansion. This results on:

$$((\mathbf{I} + \theta\hat{\varepsilon})\, X_i)_{3\times 1} \times n_i - m_i = 0 \qquad (2)$$

which can be ordered into a set of linear equations equation of the form $\mathbf{A}\varepsilon = \mathbf{b}$. The least-squares estimation of this over-determined set of linear equations is calculated by singular value decomposition or by QR factorization using Householder reflections. The Rodriguez formula is then applied to reconstruct **M** from the twist ε. Then, the new estimations of 3D points X_i can be projected again and the process is iterated until the gradient descent approach converges.

This iterative procedure can be trapped in local minima, so we use a sampling method with different start poses and use the resulting pose with minimum error.

2.4. Matching of angiograms

The bed movement between angiograms prevents that a unique rigid transform applied over the SI map is valid for all views. Additionally, respiratory and cardiac motion are major challenges leading to misalignments between angiograms. So, the end-diastolic frame and the same respiratory phase (estimated from the catheter and diaphragm motion) are selected in the fusion process to reduce this effect.

Instead of repeating the 3D-2D registration between model points X_i and image points x_i for every angiogram, a relative orientation problem is proposed: The recovery of the position and orientation of one imaging system relative to another from correspondences between projections. The solution can be computed for calibrated cameras by solving a set of simultaneous linear equations with eight matched points. Non linear methods that require at least five points have been proposed for full-calibrated cameras but the solution is not unique [9].

This number of matched points is greater than or equal to the number needed in proposed algorithm for the exterior orientation problem, but, if we assume that the bed movement only implies a translation, and the primary and secondary angles (i.e., relative rotation between views) are known, only the relative translation vector needs to be estimated. This relative orientation problem can be solved by matching only two points in each view [10].

2.5. Fusion with ventriculograms

The registration procedure is optionally combined with an iterative closest point algorithm (ICP) that aligns the ventricular contours from two ventriculograms in right anterior oblique (RAO) and left anterior oblique (LAO) views with the SI map.

Initial registration of the surface data and the two dimensional contours was initially accomplished using the left ventricular apex and the two mitral annulus points in the LAO view. In the RAO view, only mitral points were selected. These five image points x_i distributed in two aligned views are enough to perform an initial estimation of the relative orientation problem [6]. Note that equation (2) is also applicable if Plücker lines are calculated from different camera poses.

The refined registration is then calculated using a surface-to-contour ICP algorithm [11] to match the 3D ventricular mesh with the two contours of the segmented ventriculograms in LAO and RAO views.

2.6. Software implementation

The registration algorithm and visualization of results have been implemented in a user friendly graphical user

interface (GUI), which allows to navigate across the 3D data sets and visualize both MRI data and SI maps, as well as relative position and orientation of the C-arm. In Figure 1, an example with a SI map and model points X_i is shown.

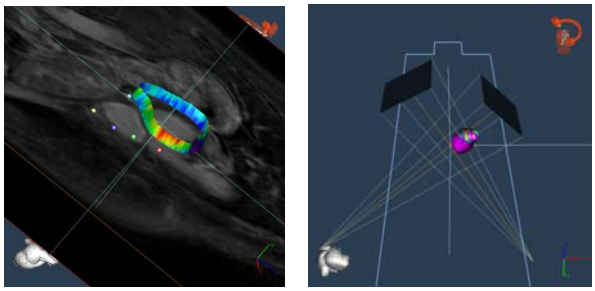

Figure 1. *Right*: Screenshots of the GUI showing the relative pose of the C-arm in two angiograms and the colored SI map. *Left*: Detail of a ventricular SI map overlapped to the ceMRI data and selected points X_i.

3. Experiments and results

ceMRI images were acquired with a 1.5T Philips Intera scanner. Left ventricular angiographies in typical orientations were acquired using a Siemens Axiom-Artis system.

The proposed methods were tested in clinical datasets from 6 patients with prior myocardial infarction. A maximum number of 5 points (apex, coronary junctions, bony structures and catheter) were identified in each ceMRI and their correspondence in one angiogram. A sample of results is shown in Figure 2: In the left column, fusion prior to registration is shown, together with the internal markers selected by the user. In the right column, the fused SI maps were registered. The distance between the manually selected marker and the projection s of the associated 3D point (plotted as an asterisk) is the projection error. Figure 2 displays the following views:

(a.1-2):RAO caudal (PA:-20º, SA:-18.5º) LCA
(b.1-2): AP cranial (PA=7º, SA=26º), RCA
(c.1-2): LAO cranial (PA=45º, SA=27º), LCA
(d.1-2): AP (PA=0º, SA=0º), RCA

The endocardial SI map is fused in images (a-b), while epicardial SI map is shown in images (c-d).

The root mean square value of the projection error had a mean value of 12.2 pixels, ranging from 21 pixels in the worse study, to 5.5 pixels.

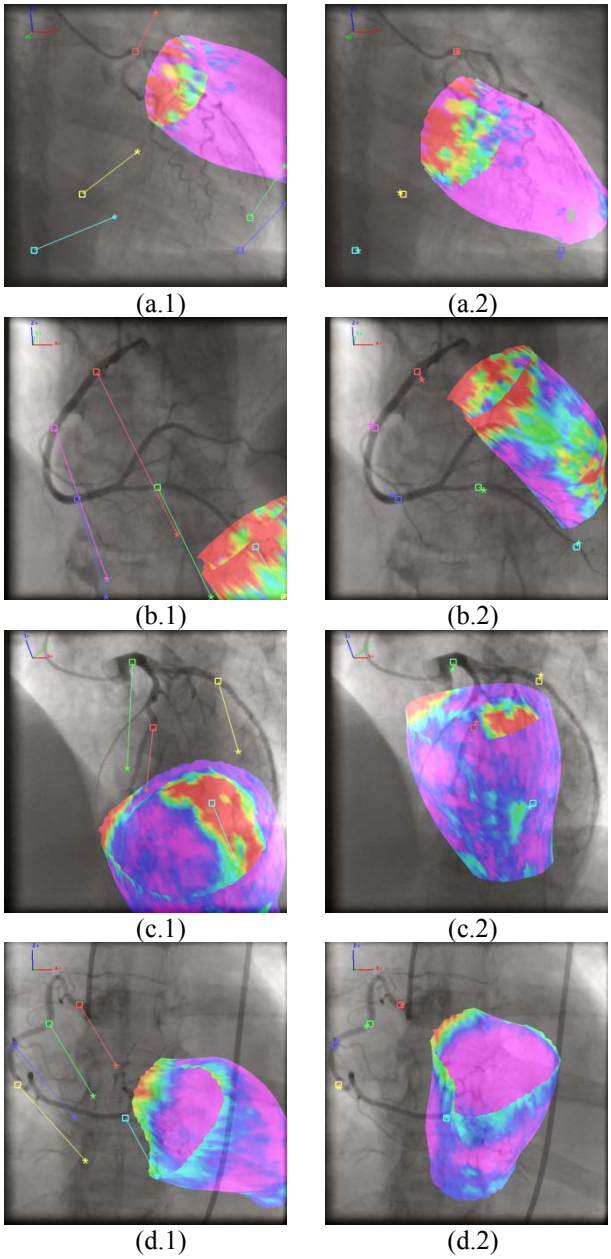

Figure 2. Fused results of X-ray angiograms and SI maps.

Additionally, the combination with the ICP algorithm was tested with acquired ventriculograms. In Figure 3, RAO view (PA=-30º) is shown in the images of the right column, and LAO view (PA=45º) in the left column. Images (a.1-2) show the fusion of the endocardial SI map before the registration process. Three points were selected in the RAO view (apex, and two mitral valve points) and two points in the LAO view. The initial point-based registration results are exhibited in images (b.1-2), which are refined with the surface-to-contour ICP based algorithm in images (c.1-2)

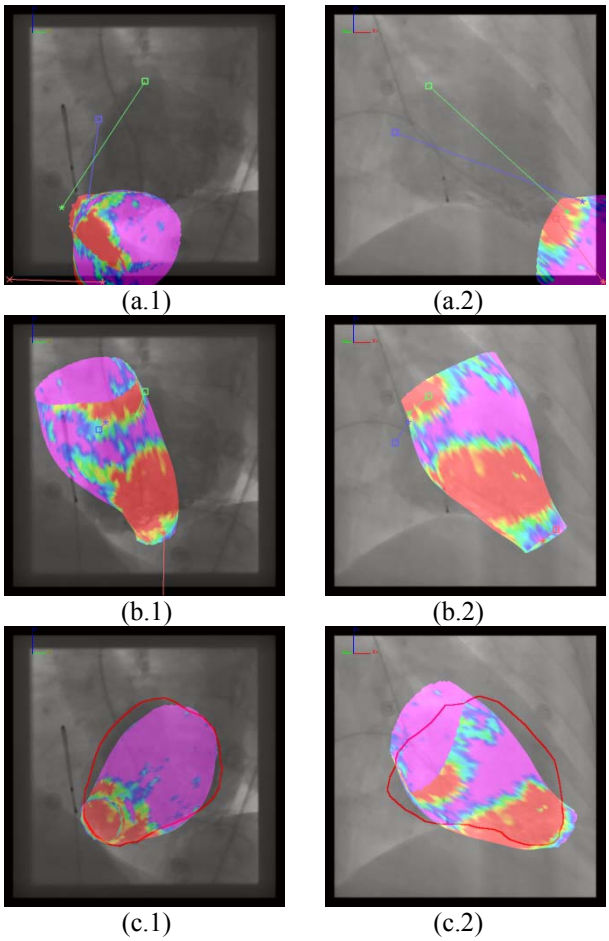

Figure 3. Fusion of ventriculograms with endocardial SI maps.

4. Discussion and conclusion

Internal marker-based 2D-3D registration has proven to be robust and able to be performed correctly. Additionally an ICP contour to surface strategy has been combined to provide a more flexible data-input. The proposed methods provide a flexible solution for typical clinical settings with promising clinical relevance. Fusion results were validated by experts in cardiac imaging and intervention.

Acknowledgements

This work was partially supported by the National Fund for Health Research (Fondo de Investigación Sanitaria) grant PI10/02771, Ministry of Science & Innovation through project TEC2010-21619-C04-03, Comunidad de Madrid (ARTEMIS S2009/DPI-1802) and Cooperative Cardiovascular Disease Research Network (RECAVA), Instituto de Salud Carlos III, Ministry of Health, Spain.

CIBER-BBN is an initiative funded by the VI National R&D&i Plan 2008–2011, Iniciativa Ingenio 2010, Consolider Program, CIBER Actions, and financed by the Instituto de Salud Carlos III with assistance from the European Regional Development Fund.

References

[1] de Silva R, Gutierrez LF, Raval AN, McVeigh ER, Ozturk C, Lederman RJ. X-ray fused with magnetic resonance imaging (XFM) to target endomyocardial injections: Validation in a swine model of myocardial infarction. Circulation 2006; 114(22):2342-50.

[2] Perez-David E, Arenal A, Rubio-Guivernau JL, del Castillo R, Atea L, Arbelo E, et al. Noninvasive Identification of Ventricular Tachycardia-Related Conducting Channels Using Contrast-Enhanced Magnetic Resonance Imaging in Patients With Chronic Myocardial Infarction. J Am Coll Cardiol 2011; 57(2):184-94.

[3] Gutierrez LF, de Silva R, Ozturk C, Sonmez M, Stine AM, Raval AN, et al. Technology preview: X-ray fused with magnetic resonance during invasive cardiovascular procedures. Catheter Cardio Inte 2007; 70(6):773-82.

[4] Rubio-Guivernau JL, Perez-David E, Arenal Á, Bermejo J, Santos A, Ledesma-Carbayo MJ. 3D visualization of myocardial substrate using Delayed Enhancement MRI for pre-planning and guidance of ablation procedures of ventricular tachycardia. J Cardiov Magn Reson 2011; 13 (Suppl 1):O56.

[5] Wu YH, Hu ZY. PnP problem revisited. J Math Imaging Vis. 2006; 24(1):131-41.

[6] Moreno-Noguer F, Lepetit V, Fua P, editors. Accurate Non-Iterative O(n) Solution to the PnP Problem. IEEE 11th International Conference on Computer Vision (ICCV 2007); 2007 14-21 Oct.; Rio de Janeiro, Brazil.

[7] Brox T, Rosenhahn B, Weickert J. Three-dimensional shape knowledge for joint image segmentation and pose estimation. Pattern Recognit 2005; 3663:109-16.

[8] Murray R, Li Z, Sastry S. A mathematical introduction to robotic manipulation. Boca Raton, FL: CRC Press; 1994.

[9] Kukelova Z, Bujnak M, Pajdla T. Polynomial Eigenvalue Solutions to the 5-pt and 6-pt Relative Pose Problems. In: Everingham M, Needham C, editors. Proceedings of the British Machine Vision Conference; Leeds: BMVA Press; 2008. p. 56.1-.10.

[10] Sun CM. 2-Point linear algorithm for camera translation vector estimation with known rotation. Robotica 2000; 18:557-61.

[11] Feldmar J, Ayache N, Betting F. 3D-2D projective registration of free-form curves and surfaces. Comput Vis Image Und 1997; 65(3):403-24.

Address for correspondence.

Juan E Ortuño Fisac.
Dpto. de Ingeniería Electrónica
E.T.S.I. Telecomunicación. Univ. Politécnica de Madrid
Avenida Complutense 30, "Ciudad Universitaria"
E-28040 Madrid (Spain).
juanen@die.upm.es